ORIGINAL ARTICLE

Combination therapy with miR34a and doxorubicin synergistically inhibits Dox-resistant breast cancer progression *via* down-regulation of Snail through suppressing Notch/NF-κB and RAS/RAF/MEK/ERK signaling pathway

Xiaoxia Yang, Pengfei Shang, Bingfang Yu, Qiuyang Jin, Jing Liao, Lei Wang, Jianbo Ji, Xiuli Guo[*]

Department of Pharmacology, Key Laboratory of Chemical Biology (Ministry of Education), Drug Screening Unit Platform, School of Pharmaceutical Sciences, Shandong University, Jinan 250012, China

Abstract   Resistance to breast cancer (BCa) chemotherapy severely hampers the patient's prognosis. MicroRNAs provide a potential therapeutic prospect for BCa. In this study, the reversal function of microRNA34a (miR34a) on doxorubicin (Dox) resistance of BCa and the possible mechanism was investigated. We found that the relative level of miR34a was significantly decreased in Dox-resistant breast cancer cell MCF-7 (MCF-7/A) compared with Dox-sensitive MCF-7 cells. Transfection with miR34a significantly suppressed the invasion, migration, adhesion of MCF-7/A cells without inhibiting their growth obviously. The combination of miR34a and Dox could significantly inhibit the proliferation, migration, invasion and induce the apoptosis of MCF-7/A cells. The synergistic effect of this combination on resistant MCF-7/A cells has no obvious relation with the expressions of classical drug-resistant proteins P-GP, MRP and GST-π, while closely related with the down-regulation on TOP2A and BCRP. Moreover, we found both protein and mRNA expression of Snail were significantly up-regulated in MCF-7/A cells in comparison with MCF-7 cells. Transfection with small interfering RNA (siRNA) of Snail could inhibit the invasion, migration and adhesion of drug-resistant MCF-7/A cells, while high-

expression of Snail could remarkably promote the invasion, migration and adhesion of MCF-7 cells, which might be related with regulation of N-cadherin and E-cadherin. Transfection with miR34a in MCF-7/A cells induced a decrease of Snail expression. The potential binding sites of miR34a with 3′ UTR of Snail were predicted by miRDB target prediction software, which was confirmed by luciferase reporter gene method. Results showed that the relative activity of luciferase was reduced in MCF-7/A cells after co-transfection of miR34a and wild type (wt)-Snail, while did not change by co-transfection with miR34a and 3′ UTR mutant type (mut) Snail. Combination of miR34a and Dox induced a stronger decrease of Snail in MCF-7/A cells in comparison to miR34a or Dox treatment alone. What' more, for the first time, we also found miR34a combined with Dox could obviously inhibit the expression of Snail through suppressing Notch/NF-κB and RAS/RAF/MEK/ERK pathway in MCF-7/A cells. *In vivo* study indicated that combination of miR34a and Dox significantly slowed down tumor growth in MCF-7/A nude mouse xenograft model compared with Dox alone, which was manifested by the down-regulation of Snail and pro-apoptosis effect in tumor xenografts. These results together underline the relevance of miR34a-driven regulation of Snail in drug resistance and co-administration of miR34a and Dox may produce an effective therapy outcome in the future in clinic.

1. Introduction

Breast cancer (BCa), one of the frequently diagnosed malignant carcinoma, was considered to be one of the most commonly murderer of tumor-related death among women. In recent years, although the survival rate of BCa patients has improved to a certain extent and the recurrence rate has also decreased significantly, chemotherapy resistance is still the most important factor affecting the recurrence and reduction of overall survival rate of BCa patients. Major challenges of therapy for BCa patients are associated with high level of tumoral heterogeneity, distant metastases, and so on, which resulted chemotherapy resistance becoming the most serious problem that hinders tumor chemotherapy and prognosis[1,2]. Doxorubicin (Dox) is an anthracycline antitumor drug, which inhibits the growth of tumor cells mainly by targeting topoisomerase II (TOP 2A). Although Dox is a first-line chemotherapy drug for breast cancer in clinic, its inhibitory effect is not complete, especially for the patients in the late stage of BCa. Once the BCa cells develop resistance, invasion and metastasis are more likely to occur. Therefore, how to effectively reverse the resistance of BCa toward Dox and improve the clinical symptoms of BCa patients have become a top priority.

Currently, there are three commonly used methods to reverse drug resistance in clinical practice: 1) application of chemotherapy sensitizers[3] (such as inhibitors of P-GP, verapamil); 2) traditional Chinese medicine monomer reversal agents[4] (such as tetrandrine, ligustrazine, matrine, emodin, etc.); 3) gene reversal agents[5] (such as RNA interference, microRNA, etc.). Most chemotherapeutic sensitizers and traditional Chinese medicine monomers have serious toxic and side effects due to the large dose required to achieve effective reversal, and their effects are relatively complex, which limits their further investigation and clinical application. Therefore, the use of small molecular gene regulators such as microRNA (miR) to reverse drug resistance has become a research focus in recent years.

miR, which are of about 18−25 nucleotides size, mainly involved in regulating the expression of target gene[6]. They partially bind with 3′ un-translated regions (UTRs) of target mRNA, leading to a suppression effect on the specific protein. miR expression imbalance is associated with a multitude of diseases including BCa. And miR may also play a key role in chemotherapy resistance in BCa. microRNA34a (miR34a) has been proven participating in the genesis and development of various tumors through multiple targets such as BCL-2, CD44, c-MET, SIRT1, CDK, MYC, etc[7]. Recent studies showed that miR34a could abrogate urothelial bladder cancer chemoresistance *via* regulating Golgi phosphoprotein 3[8]. Up-regulation of miR34a might be a viable therapeutic agent for castration-resistance prostate cancer[9]. And miR34a decreases the chemoresistance of colon cancer toward 5-FU through targeting E2F3 and SIRT1. The above studies indicated there is a correlation between miR34a and chemoresistance.

Therefore, in this study, we intended to explore whether miR34a could reverse Dox resistance in BCa, and proposed the hypothesis that miR34a could be used in combination with Dox for treating metastatic BCa, and then elucidated the possible molecular mechanism and related signaling pathways.

2. Materials and methods

2.1. Cell culture

The human breast cancer cell line MCF-7, Dox-resistant breast cancer cell line MCF-7 (termed MCF-7/A), human umbilical vein endothelial cells (HUVECs), were acquired from National Collection of Authenticated Cell Cultures (Shanghai, China). HUVECs were routinely cultured in RPMI 1640 medium (Thermo Fisher Scientific, Inc., USA), supplemented with 1% penicillin/streptomycin (Meilunbio, Dalian, China) and 10% fetal bovine serum (FBS; HONBIOTECH, China) in a humidified incubator at 37 °C with 5% CO_2. MCF-7 and MCF-7/A cells were cultured in RPMI-1640 medium plus 1% penicillin/streptomycin, 10% FBS and insulin (2 mg/mL, Dalian Meilun Co., Ltd., China) in a humidified 5% CO_2 incubator at 37 °C.

2.2. In vitro cell transfection

Has-miR34a mimics (miR34a), hsa-miR negative control (NC), Snail siRNA was obtained from Genepharm Co., Ltd. (Shanghai,

China). Over-expression plasmid of Snail was constructed by Jinan Weizhen Co., Ltd. MCF-7/A cells in exponential phase were spread in a 6-well plate and cultured to 60% confluence before transfection. Micropoly (Nantong Michaelui Biotechnology Co., Ltd.) was used as a transfection reagent, because of the less cytotoxicity compared to routine transfection reagents (Lipo2000 and 3000) and highly effective cell transfection for DNA/RNA transfection[10]. miR34a/Snail siRNA, over-expression plasmid of Snail or NC were gently mixed with micropoly, leave for 10 min, and were added into the culture medium. Then cells were incubated for 24 h at 37 °C for further treatment.

The sequence of miR or siRNA are displayed as follows:
miR34a, 5′−3′: UGGCAGUGUCUUAGCUGGUUGU.
NC, 5′−3′: UUCUCCGAACGUGUCACGUTT.
Snail siRNA, 5′−3′: GGCCUUCAACUGCAAAUAUTT.

2.3. Cell viability analysis

MTT assay was employed to analyze the viability of MCF-7/A cells. Cells (5000 cells/well) were spread into a 96-well plate, and 24 h later, cells were transfected with miR34a at different concentrations (50, 100, and 150 nmol/L), and Dox at different concentrations for 48 h. Then MTT solution was added into the wells and incubated for 4 h at 37 °C and the purple crystals were dissolved with DMSO. The absorbance was determined at 570 nm employing the microplate reader (Thermo Multiskan GO, USA).

2.4. Hoechst 33342 staining assay

MCF-7/A cells (5×10^4 cells/well) were spread into a 24-well plate and administrated with miR34a and/or Dox for 48 h, then methanol-glacial acetic acid (3:1, v/v) was added and cells were stained for 15 min with Hoechst 33342. After washed with PBS, cells were photographed under a fluorescence microscope (200×, TE2000-S, Japan).

2.5. Annexin V-FITC/PI staining assay

MCF-7/A cells were paved into a 6-well plate (4×10^5 cells/well) before administrated with miR34a and/or Dox for 48 h. Then cells were collected, washed with PBS and were dual-stained with an Annexin V-FITC/PI detection kit (Beyotime Biotechnology, Shanghai, China) following the manufacturer's protocols. Stained cells were immediately analyzed with a FACScan flow cytometry (Becton Dickinson, USA).

2.6. Wound scratch assay

MCF-7 and MCF-7/A cells (5×10^5 cells/well) was paved into a 6-well plate and grew until 80%−90% confluence monolayer was obtained. A mechanical wound was gently created to produce a scratch with a pipette tip. After administration with miR34a and/or Dox, images of cells were taken at 0, 24 and 48 h, respectively, after wounding employing the inverted fluorescence microscope.

2.7. Cell Transwell migration and matrigel invasion assay

Transwell assay was employed to evaluate the changes of cell migratory and invasive abilities after treatment with miR34a and/or Dox. Collected cells were resuspended in medium without serum, 50,000 counted cells were spread into the upper chamber and complete medium containing 20% FBS was put into the lower compartment. 48 h later, cells that passed through the chamber were fixed with glacial acetic acid, stained with crystal violet (0.08%, v/v), and were photographed by taking six random fields of per well under a fluorescence microscope. For the invasion assay, Matrigel was firstly spread into the Transwell membrane and incubated for 1 h, and the rest of procedures were similar to the migration assay.

2.8. Cancer cell−endothelial cell adhesion assay

Cancer cell−endothelial cell adhesion assay was employed as reported previously with a few changes[11]. MCF-7/A cells cultured in complete medium were spread in a 6-well plate, while HUVECs was seeded in a 24-well plate. miR34a or Snail-siRNA, NC were transfected into tumor cells for 24 h. Then the transfected cells were collected, counted and resuspended into serum-free 1640 medium allowing dying with 5 μmol/L DIO dye for 30 min. After that, equal amounts of stained cells from different groups were spread above HUVEC cells in the 24-well plate and incubated at 37 °C for 40−50 min. Then the non-adherent tumor cells were gently washed away with PBS. Finally, fluorescence microscopy was used to randomly select 10 fields for photography of adherent cells (100 magnifications).

2.9. Quantitative real-time PCR (qRT-PCR)

Cells were transfected with micropoly for 24 h. RNA was extracted and complementary DNA (cDNA) was reverse-transcribed with a specific miR34a/U6 RT primer. RT-PCR was performed with a LightCycler 480 Detection system (Roche, Switzerland). The primers for miR34a/U6 or Snail/β-actin were displayed in Supporting Information Table S1. The reaction solution of a 20 μL system contained 10 μL of SYBR Green Realtime PCR Master Mix, 6.4 μL of distilled water, 1.6 μL of primers (upstream and downstream, 10 μmol/L) and 2 μL of cDNA. The conditions for PCR cycle are performed as follows: denaturation at 95 °C for 5 min, followed by 40 cycles of denaturation at different temperatures (95 °C for 5 s, 55 °C for 10 s and 72 °C for 15 s). The relative expression level of miR34a or Snail was normalized to the internal control U6 or β-actin.

2.10. miR34a target gene identification

miRDB (http://mirdb.org/) and starbase (http://starbase.sysu.edu.cn/) was used to search the target genes of miR34a.

2.11. Dual luciferase activity assay

To verify the precise target of miR34a, dual luciferase assay was performed in MCF-7/A cells. Cells were spread into a 24-well plate until 80% confluence was reached before transfection. The wild-type (wt) 3′ UTR (which contain the putative target site with miR34a) and mutant-type (mut) 3′ UTR of Snail were constructed into pmirGLO vector (Jinan Bo Shang Co., Ltd.). 500 ng (w/w) Snail-3′ UTR and mut Snail-3′ UTR vector together with 50 nmol/L NC or miR34a were co-transfected with micropoly into MCF-7/A cells for 48 h. Then the Firefly and Renilla luciferase activity were determined employing a Firefly & Renilla Luciferase Reporter Assay Kit (Dalian Meilun Co., Ltd., China) with a Microplate Luminometer (LB96, Berthold). The

results for the relative luciferase activity ratios were set as the *Firefly* luciferase/*Renilla* luciferase values for each sample.

2.12.   Western blotting assay

MCF-7 and MCF-7/A cells planted in 6-well plates were treated with miR34a and/or Dox for 48 h (5×10^5/well). Then cells were lysated using lysis containing 1% proteinase inhibitors (PMSF) and total protein was extracted. The concentrations were measured employing a BCA protein kit (Thermo Scientific, USA). After electrophoresis with SDS-PAGE gel was completed, the extracted proteins were transferred for 1 h (or 1.5 h) and blocked for 4 h, and then incubated with the corresponding primary antibody (Snail, E-cadherin, N-cadherin, CD44, BCL-2, PARP, Notch, pan-RAS, k-RAS, RAF, NF-κB, P-GP, GST-π, MRP1, BCRP, TOP2A, MEK1/2, ERK1/2, p-MEK1/2, p-ERK1/2 purchase from Affinity Co., Ltd., China) overnight. On the next day, the membrane was washed with TBST and incubated with secondary antibody for 1 h, and were imaged in the presence of ECL luminescent solution using Chemidoc XRS imaging system (Bio-Rad, USA).

2.13.   Immunofluorescence assay

MCF-7/A cells (5×10^3/well) was spread into a 24-well plate and grew to 80% confluence. Cells were transfected with miR34a/Snail siRNA/Snail plasmid or added with Dox alone or combined treatment with miR34a and Dox for 48 h. Fixative solution was added and cells were incubated for 10 min. After washing with PBS, 3% Triton-X permeabilization treatment on cells was performed for 10 min, and then sealed with 3% BSA for 1 h. After washing with TBST for 2–3 times, immunofluorescent dilution containing primary antibody was added and samples were incubated at 4 °C overnight for more than 24 h. Then the secondary antibody was added and incubated for 1 h, anti-fluorescence quenching agent containing DAPI was added for several seconds, cells photographs were immediately taken under a fluorescence microscope or a laser confocal microscope.

2.14.   Tumor xenograft assay

Female BALB/c nude mice (5–6 weeks old, 18–20 g) were acquired from SiPeiFu (Beijing) Biotechnology Co., Ltd. and were housed under conditions without pathogen. The experiment protocols were performed following the regulation of Welfare Committee and the Animal Care of Shandong University. MCF-7/A xenograft were established by inoculating MCF-7/A cells (1×10^7 cells) subcutaneously in the axilla of nude mice. Once the volume of the xenograft reached 100 mm^3, well-grown tumors were extracted, cut and transplanted into the right flank of each mouse under sterile conditions. When the tumor volume reached 80–100 mm^3, mice with too large or too small tumors were excluded, and 12 nude mice with uniform shape and size were left and randomly divided into four groups ($n = 3$): (1) Control group (normal saline); (2) AgomiR34a group (2.5 nmol/L each mice every 3 days); (3) Dox group (5 mg/kg each mice every 3 days); (4) AgomiR34a (2.5 nmol/L) combined with Dox (5 mg/kg) group. miR34a was administrated through intratumor injection in the form of agomiR34a while Dox was administrated through tail vein injection. AgomiR34a is a chemically modified form of miR34a, which is a stable structure formed by cholesterol

modification and thio skeleton modification, and can be administered by systemic injection or local injection[12]. Tumor size and body weight was determined every 3 days using Vernier calipers for 21 days. The tumor volume (mm^3) was calculated as $0.5 \times$ length $\times$ width^2. About 3 weeks later, the mice were sacrificed, and tumors were separated, weighed and frozen for immunofluorescence/immunohistochemical evaluation.

2.15.   Statistical analysis

All experiments were performed and repeated at least three times. Data were set as the mean value $\pm$ standard deviation (SD) and analyzed by Graph Pad Prism 5.0. Student's *t*-test was employed to calculate the significance difference between different groups. $P < 0.05$ is considered statistically significant.

3.   Results

3.1.   Dox-resistant MCF-7/A cells showed stronger invasion, metastasis and adhesion abilities than Dox-sensitive MCF-7 cells

Compared with Dox-sensitive MCF-7 cells, Dox-resistant MCF-7/A cells showed a stronger ability of invasion and migration, and a higher adhesion ability with HUVEC cells (Fig. 1A and B). Moreover, the expressions of proteins associated with invasion and migration were detected, and we found that the expressions of N-cadherin and CD44 were significantly increased while E-cadherin expression was significantly decreased in Dox-resistant cells (Fig. 1C), indicating that MCF-7/A cells are more prone to invade, migrate and adhere to endothelial cells than MCF-7 cells, which might be related to a decreased expression of E-cadherin and an increased expression of N-cadherin and CD44.

3.2.   Transfection of miR34a suppressed the proliferation, invasion and migration of MCF-7/A cells and adhesion to HUVECs

To investigate whether there existed different expressions of miR34a between MCF-7 and MCF-7/A cells, qRT-PCR was firstly performed and the result verified miR34a expression in MCF-7/A cells was dramatically decreased in comparison with that in MCF-7 cells ($P < 0.001$, Fig. 2A). To further understand the effect of miR34a on the function of MCF-7/A cells, we conducted transfection *in vitro* with micropoly and successfully over-expressed miR34a in MCF-7/A cells (Fig. 2B). Cells were cultured with miR34a at different concentrations (25, 50, and 100 nmol/L) and the cell viability after miR34a transfection was slightly decreased (Fig. 2C), whereas the migration, invasion and adhesion to HUVECs of MCF-7/A cells were obviously inhibited with the increase of miR34a concentration (Fig. 2D). Further scratch experiments *in vitro* also confirmed that cell migration was inhibited at a high concentration of miR34a (Fig. 2E). Furthermore, the expressions of EMT related proteins were detected after transfection with miR34a in MCF-7/A cells, and results showed the protein levels of N-cadherin and CD44 were down-regulated, while the level of E-cadherin was up-regulated in comparison to blank control (BC) and negative control (NC), indicating that the suppression effect of miR34a on the invasion, migration and adhesion of MCF-7/A cells was related to
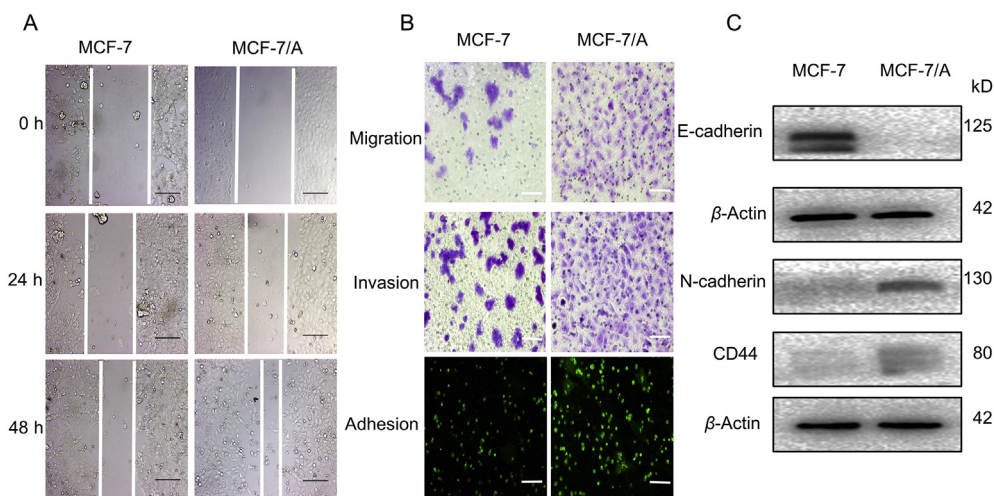
Figure 1 Differences between Dox-sensitive MCF-7 cells and Dox-resistant MCF-7/A cells. (A) Wound scratch assay was employed to compare the migration difference between MCF-7 and MCF-7/A cells. (B) Transwell assay was used to compare the invasion and migration ability between MCF-7 and MCF-7/A cells. Adhesion ability of MCF-7 or MCF-7/A cells with HUVEC cells was detected by adhesion assay. (C) Expression differences of EMT-related proteins (N-cadherin, E-cadherin, CD44) between the MCF-7 and MCF-7/A cells were determined by Western blotting assay. Scale bar = 20 μm.

the regulation of E-cadherin/N-cadherin and CD44 molecules (Fig. 2F).

3.3. miR34a enhanced the susceptibility of MCF-7/A cells to Dox through inhibiting the proliferation and promoting the apoptosis

Firstly, the fold change of resistance between MCF-7 cells and MCF-7/A cells was calculated after the IC_{50} values of Dox on sensitive MCF-7 and Dox-resistant MCF-7/A cells were detected. Results indicated that the IC_{50} of Dox on MCF-7 cells and MCF-7/A cells was 4.25 and 106.7 μmol/L, respectively, thus the resistance of MCF-7/A is 24.98-fold of MCF-7 cells.

Next, the IC_{50} of Dox on MCF-7/A cells after combination treatment with different concentrations of miR34a (25, 50 and 100 nmol/L) for 48 h was measured and results showed that as the increase of miR34a concentration, the IC_{50} of Dox in the co-administration group decreased significantly, from 106.17 to 41.35, 29.28 and 14.08 μmol/L. Then the reversal multiple (also called the synergy index, R) was calculated by the formula that is the IC_{50} of Dox alone divide by the IC_{50} of Dox in combination with miR34a. $R > 1$ indicates a synergistic effect for Dox combined with miR34a. $R \leq 1$ indicates that there is no synergistic effect between Dox and miR34a. The calculated R values for the combination of Dox and miR34a (25, 50 and 100 nmol/L) are 2.57, 3.63 and 7.54, respectively, indicating that there existed a dramatically synergistic effect of the combination treatment (Fig. 3A). The above results indicated that miR34a could improve the sensitivity of Dox toward resistant MCF-7/A cells.

Based on the above results, 100 nmol/L miR34a combined with different concentrations of Dox achieved the maximum reversal multiple (synergism index) which is 7.54, so 100 nmol/L miR34a was chosen for the combination treatment in the subsequent experiments. Moreover, the concentration of Dox for the combination treatment was decided to be 10 μmol/L which is lower than the IC_{50} of Dox on MCF/A cells when combined with miR34a at 100 nmol/L which was 14.08 μmol/L. The results of

MTT assay indicated that after treatment of Dox at 10 μmol/L combined with different concentrations of miR34a (25, 50, and 100 nmol/L), the inhibition rates on the survival of MCF-7/A cells increased from 20% (Dox alone) to 27.31%, 31.85% and 40.56%, respectively (Fig. 3B).

To study the impact of this combination on the apoptosis of MCF-7/A cells, changes in cell morphology were firstly examined with Hoechst 33342 as a nuclear stain. As we can see in Fig. 3C, the combined use of miR34a and Dox can induce apoptosis with typical characteristics like nuclear fragmentation, chromatin condensation and shrinkage in comparison with control MCF-7/A cells. Then flow cytometry was further employed to quantitatively determine the percentage of apoptosis after cells were double-stained with Annexin V-FITC/PI. Results showed that co-treatment of miR34a and Dox could obviously increase the proportions of apoptotic cells (Fig. 3D and F). Subsequently, the level of apoptosis-related proteins was further verified by Western blotting, and the results indicated that the co-administration of miR34a and Dox could decrease the ratio of BCL-2/BAX by down-regulating BCL-2 and up-regulating BAX, and dramatically increase the expression of cleaved-PARP (Fig. 3E and G). These results suggested that miR34a combined with Dox exhibit a synergistic pro-apoptotic effect by decreasing the ratio of BCL-2/BAX and promoting the cleavage of PARP protein.

3.4. Combination treatment of miR34a and Dox down-regulated protein expressions of TOP2A and BCRP, without obvious impacts on the expressions of P-GP, MRP and GST-π

To investigate whether miR34a can reverse drug-resistance of breast cancer cell MCF-7/A to Dox, the levels of classical drug-resistant proteins, P-GP, MRP, GST-π, BCRP and TOP2A were examined. Results showed that MCF-7/A cells exhibited a higher level of P-GP, MRP and GST-π in comparison with sensitive MCF-7 cells. The combination treatment of miR34a and Dox didn't show significant effects on the expressions of three proteins (Fig. 4). However, it could obviously down-regulate the
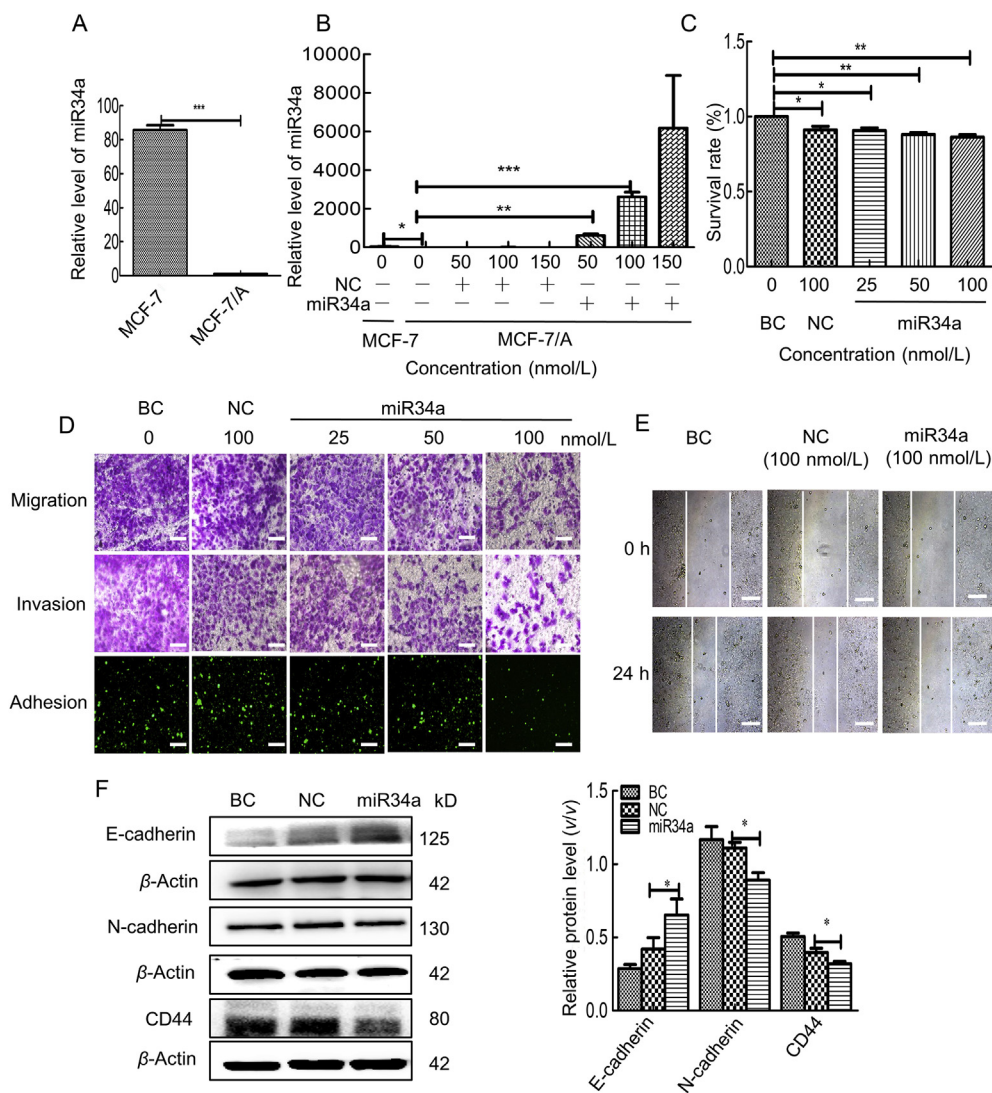
Figure 2 Transfection of miR34a inhibited the invasion, migration, and adhesion to HUVECs of MCF-7/A cells. (A) mRNA level of miR34a in MCF-7/A cells or MCF-7 cells was detected by qRT-PCR. (B) mRNA level of miR34a after transfection with miR34a mimics at different concentrations in MCF-7/A cells was detected by qRT-PCR. (C) Effects of miR34a at different concentrations on the proliferation were determined by MTT assay in MCF-7/A cells. (D) Effects of miR34a at different concentrations on the invasion, migration and adhesion to HUVECs of MCF-7/A cells were detected. (E) The migration of MCF-7/A cells after transfection with miR34a at 100 nmol/L was detected by wound scratch test. (F) The expression levels of EMT-related proteins (N-cadherin, E-cadherin, CD44) after transfection with miR34a for 48 h in MCF-7/A cells were detected by Western blotting assay and the relative protein ratios were analyzed statistically ($n \geq 3$). *$P < 0.05$, scale bar = 20 μm.

expressions of BCRP and TOP2A in MCF-7/A cells, suggesting that the reversal of miR34a on Dox resistance in breast cancer cells might be associated with the down-regulation of BCRP and TOP2A.

3.5. Co-administration of miR34a and Dox inhibited the invasion and migration phenotype of MCF-7/A cells via regulating the protein level of E-cadherin and N-cadherin

The effect of co-administration of miR34a and Dox on the invasion and migration was detected by wound-healing assay and Transwell assay in MCF-7/A cells. In order to reduce the impact on cell proliferation, we selected 7 μmol/L Dox and 100 nmol/L miR34a for combined experiments. In wound healing assay, compared with MCF-7 cells, MCF-7/A cells displayed a faster

healing ability, indicating MCF-7/A cells are more likely to migrate. However, after transfection of miR34a, the migration rate of MCF-7/A cells was inhibited. What's more, the combination of miR34a and Dox induced a stronger inhibition on the wound healing of MCF-7/A cells than Dox alone at 48 h (Fig. 5A and B). In Transwell migration or Matrigel invasion assay, MCF-7/A cells have a faster migration and invasion rate than that of sensitive MCF-7 cells. miR34a obviously restrained the invasion and metastasis of drug-resistant MCF-7/A cells, while Dox alone had no significant effects on invasion and migration. However, miR34a combined with Dox remarkably inhibited the invasion and migration of MCF-7/A cells with a higher inhibition rate in comparison to untreated group and Dox or miR34a treated alone group (Fig. 5C and D). Subsequently, the effects of single or combined use on the expressions of migration associated proteins
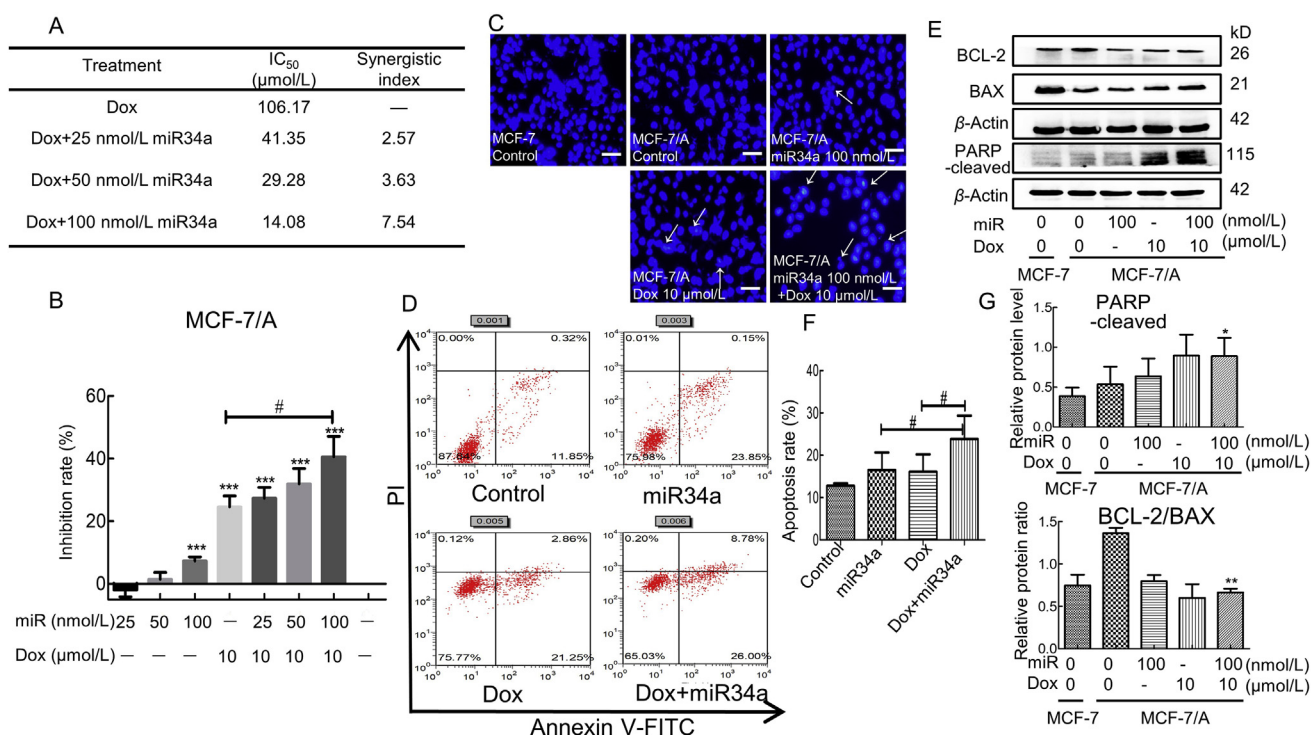
Figure 3 The combination of miR34a and Dox significantly suppressed the survival and induced the apoptosis in MCF-7/A cells. (A) The IC_{50} values of Dox on MCF-7/A cells when Dox is used alone or in combination with different concentrations of miR34a (25, 50, and 100 nmol/L) for 48 h were determined. (B) The combination of 100 nmol/L miR34a and 10 μmol/L Dox remarkably suppressed the survival of MCF-7/A cells compared with Dox alone ($n = 3$). ***$P < 0.001$ vs. untreated MCF-7/A, #$P < 0.05$ vs. Dox alone. (C) Hoechst 33342 was used to detect the effects of 100 nmol/L miR34a alone, 10 μmol/L Dox alone or a combination on MCF-7/A cell apoptosis after treatment for 48 h. Blue indicates the nucleus. Arrows indicate apoptotic cells. Scale bar = 20 μm. (D) After treatment with miR34a or Dox alone or co-administration for 48 h, MCF-7/A cells were double-stained with Annexin V-FITC/PI kit and analyzed with flow cytometer. (E) Protein levels of cleaved-PARP, BAX, BCL-2 in MCF-7/A cells were analyzed by Western blotting. (F) Quantitative analysis of apoptosis rate which included early and late apoptotic cells ($n \geq 3$). #$P < 0.05$ vs. Dox or miR34a alone. (G) The relative protein ratio of cleaved-PARP and the ratio of BCL-2/BAX were calculated ($n \geq 3$). *$P < 0.05$, **$P < 0.01$ vs. untreated MCF-7/A cells. miR represents miR34a.

in MCF-7/A and MCF-7 cells were tested by Western blotting. In Fig. 5E, compared with sensitive MCF-7 cells, N-cadherin level increased significantly, at the same time, E-cadherin level obviously decreased in MCF-7/A cells. After treatment with miR34a, the level of N-cadherin down-regulated, while the level of E-cadherin up-regulated. Moreover, the combination treatment of miR34a and Dox induced an obvious increase of E-cadherin and an obvious decrease of N-cadherin than Dox. These data indicate that the combination of Dox and miR34a restrained the invasion and migration of MCF-7/A cells through down-regulation of N-cadherin and up-regulation of E-cadherin.

3.6. Combination treatment of miR34a and Dox resulted a decrease of Snail expression and miR34a targeted Snail directly in MCF-7/A cells

Next, the effect of co-administration of miR34a (100 nmol/L) and Dox (7 μmol/L) on the localization of intracellular Snail using immunofluorescence experiments was explored. Results showed that in MCF-7/A cells, Snail was mainly spread in the nucleus and scattered in the cytoplasm. After transfection of miR34a or treatment with Dox alone, fluorescence intensity of Snail in MCF-7/A cells slightly weakened. Surprisingly, miR34a combined with Dox could significantly reduce the fluorescence

intensity of Snail in MCF-7/A cells (Fig. 6A and B). This indicated that combination of miR34a and Dox reduced the level of Snail in Dox resistant MCF-7/A cells obviously. Furthermore, the effects of Dox alone or in combination with miR34a on the expression of Snail were also detected. Result showed that combination of Dox and miR34a could significantly reduce the protein level of Snail, while Dox alone or combination of Dox and NC did not down-regulate Snail expression (Fig. 6C). These results indicate that the combination of miR34a and Dox could inhibit Snail expression in Dox-resistant MCF-7/A cells which mainly induced by miR34a.

Based on the miRDB database and starbase website (http://starbase.sysu.edu.cn/), the underlying binding sites of miR34a in the 3′ UTR of Snail were forecast (Fig. 6D). To verify the binding between miR34a and Snail, we constructed the human Snail wild type (Snail-wt-3′ UTR, including putative miR34a binding site) and mutant type (Snail-mut-3′ UTR) into the pmiRGLO vector (Fig. 6G). Compared with NC, miR34a significantly reduced the relative luciferase activity of wt-Snail 3′ UTR while no obvious decrease of mut-Snail 3′ UTR whether NC or miR34a was co-transfected (Fig. 6H). To further confirm that miR34a targets Snail directly, the effects of miR34a on protein or mRNA level of Snail were determined separately employing Western blotting and qRT-PCR. Results showed transfection of miR34a led to a
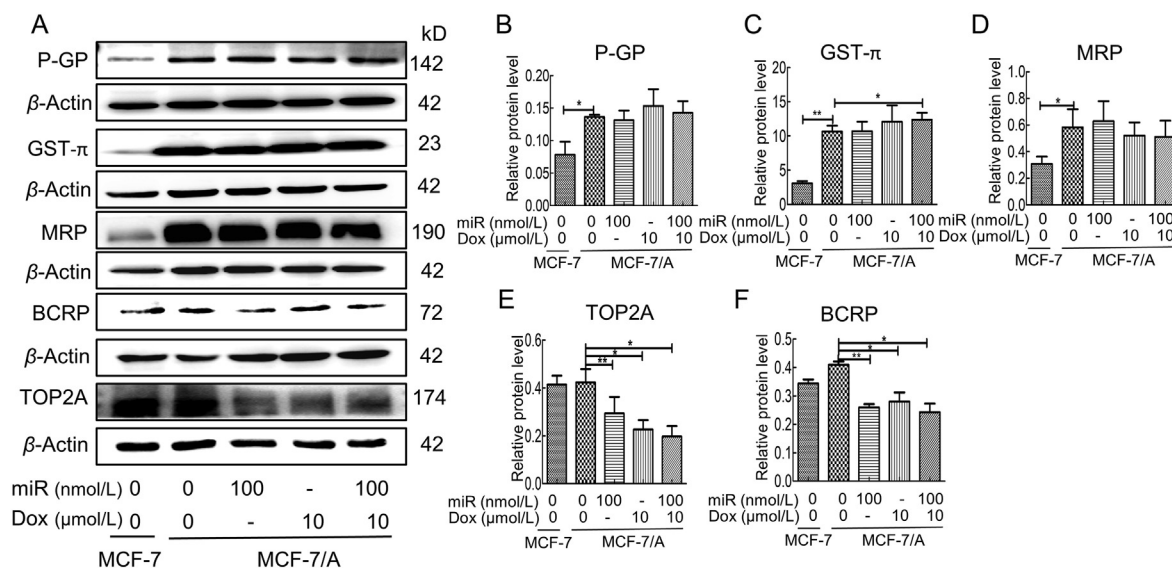
Figure 4 Effects of miR34a and Dox co-administration on the expression of drug resistant associated proteins. (A) The expressions of P-GP, GST-π, MRP, BCRP and TOP2A in MCF-7/A cells were determined by Western blotting assay. (B–F) Statistical analysis of P-GP (B), GST-π (C), MRP (D), TOP2A (E) and BCRP (F). Data are set as the mean value $\pm$ SD ($n \geq 3$). *$P < 0.05$, **$P < 0.01$, *vs.* untreated MCF-7/A cells. miR represents miR34a.
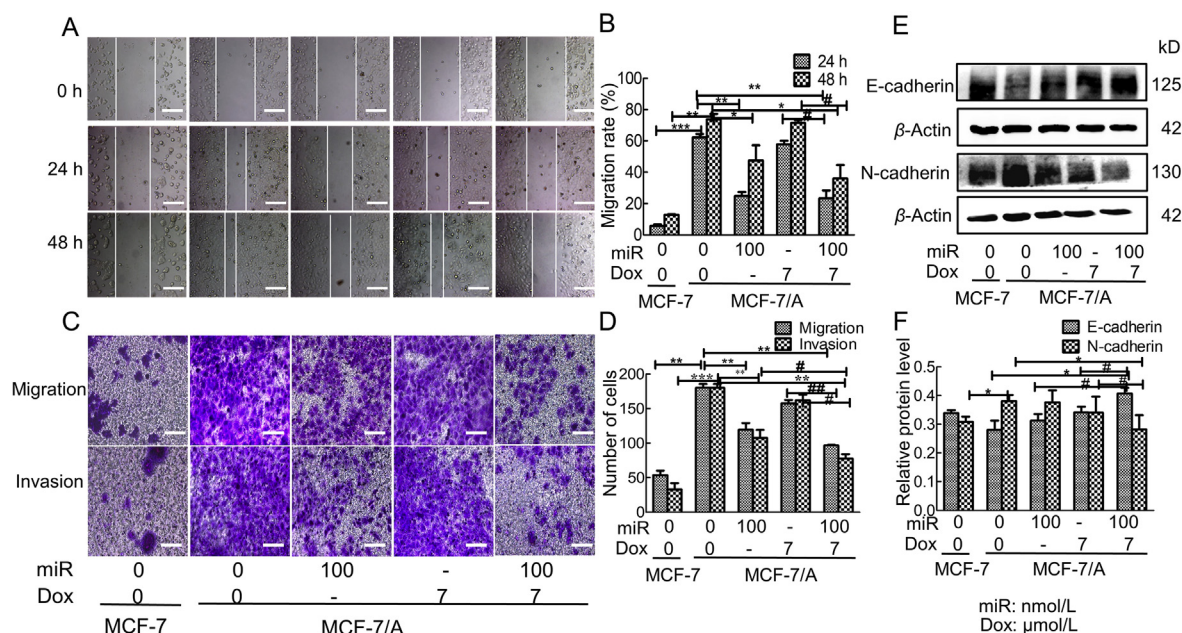

Figure 5 Combination of miR34a and Dox inhibited the migration and invasion phenotype of MCF-7/A *via* regulating the level of E-cadherin, N-cadherin. (A) After treatment with miR34a (100 nmol/L) and/or Dox (7 µmol/L), scratch test was employed to detect the changes of migration in MCF-7/A cells. Representative photographs for each group were taken under a microscopy, and the migration distance and relative mobility were calculated at 0, 24 and 48 h. (B) Statistical analysis of relative migration rate which was calculated as (width at 0 h−width at 24/48 h)/(width at 0 h) ($n = 3$), *$P < 0.05$, **$P < 0.01$, ***$P < 0.001$ *vs.* untreated MCF-7/A control, #$P < 0.05$ *vs.* Dox alone. (C) The migration and invasion capacities of MCF-7/A cells after treatment of miR34a (Dox) alone and combination were assessed by Transwell chamber assay. Representative photographs were taken under a fluorescence microscope. (D) Statistical analysis of relative migration and invasive cells ($n = 3$). **$P < 0.01$, ***$P < 0.001$ *vs.* untreated MCF-7/A control, #$P < 0.05$ *vs.* Dox or miR34a alone, ##$P < 0.01$ *vs.* Dox alone. (E) The protein levels of N-cadherin, E-cadherin were detected using Western blotting analysis. (F) Statistical analysis of protein expression. Data are expressed as the mean $\pm$ SD ($n \geq 4$). *$P < 0.05$ *vs.* untreated MCF-7/A control, #$P < 0.05$ *vs.* Dox or miR34a alone, scale bar $= 20$ µm, miR represents miR34a.
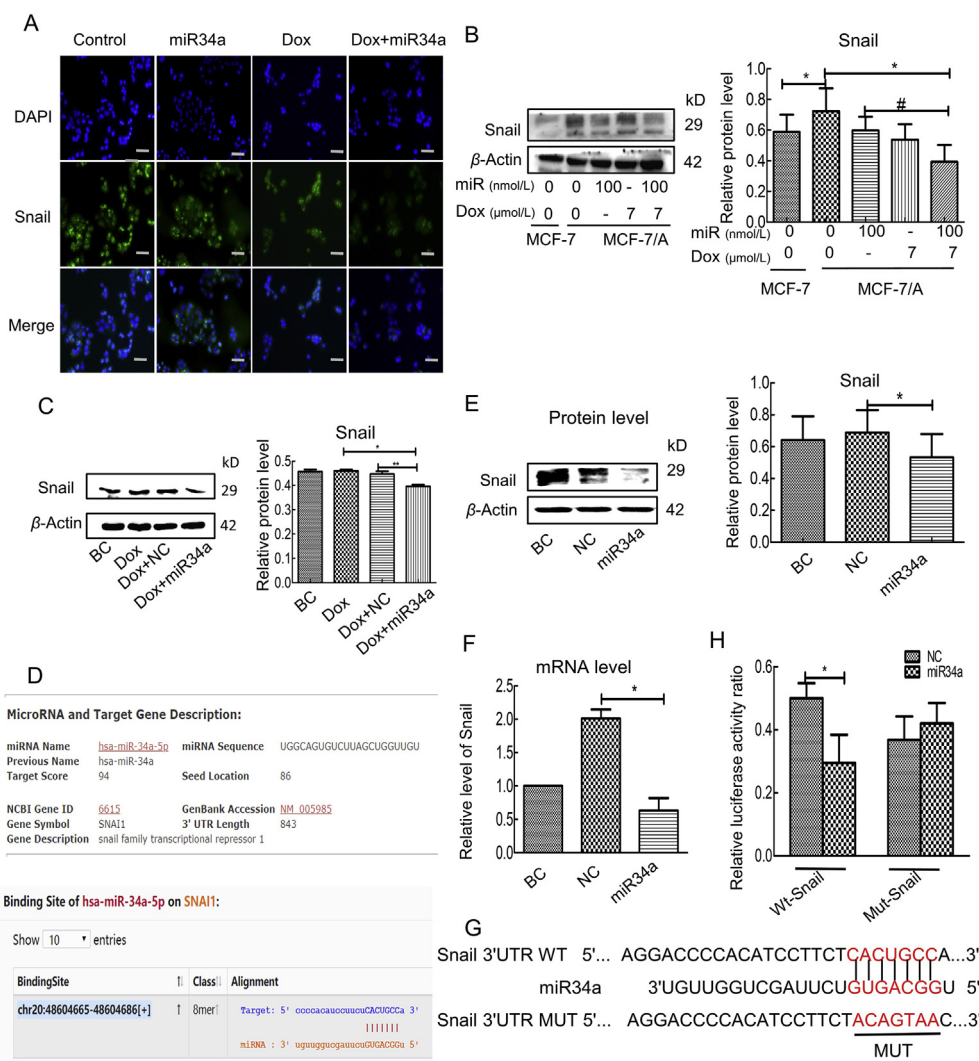
Figure 6 Combination of miR34a and Dox inhibited Snail expression and miR34a targets Snail directly in MCF-7/A cells. (A) The intracellular localization of Snail was analyzed using immunofluorescence experiments. Blue fluorescence: cell nucleus, Green fluorescence: Snail. Bar = 20 μm. (B) The expression of Snail in the two cells was determined and analyzed by Western blotting ($n \geq 3$). *$P < 0.05$ vs. untreated MCF-7/A control, #$P < 0.05$ vs. miR34a alone. (C) The expression of Snail in MCF-7/A cells after various treatments was determined and analyzed by Western blotting ($n \geq 3$). *$P < 0.05$ vs. Dox group, **$P < 0.01$ vs. Dox+NC group. (D) Binding sites between hsa-miR34a-5p and Snail were predicted by miRDB website. (E) and (F) The protein expression and mRNA level of Snail in MCF-7/A cells after transfection with miR34a and NC were detected by Western blotting and qRT-PCR ($n \geq 3$). *$P < 0.05$ vs. NC. (G) Mutant and wild type Snail fragments with putative binding sites to miR34a were constructed. (H) The binding of miR34a and Snail was determined by luciferase reporter assay using co-transfection of miR34a/NC and wt-Snail, or miR34a/NC and mut-Snail. The ratio of *Firefly* and *Renilla* luciferase signals represented relative luciferase activity. *$P < 0.05$ vs. NC. miR represents miR34a.

significant reduction of Snail at protein and gene level (Fig. 6E and F). The above experiments indicated that miR34a down-regulated the protein and gene level of Snail by binding to 3′ UTR region of Snail directly.

3.7. Down-regulation of intracellular Snail suppressed the invasion, migration and adhesion of MCF-7/A cells while over-expression of Snail promoted the invasion, migration and adhesion of sensitive MCF-7 cells.

To clarify the role of Snail involved in the proliferation, migration, invasion, and adhesion to HUVECs of drug-resistant cells, small interfering RNA of Snail (si-Snail) was introduced to suppress the level of Snail in MCF-7/A cells. Results suggested that the expression level of Snail significantly decreased in MCF-7/A cells by si-Snail which was determined by immunofluorescence assay and Western blotting assay (Fig. 7B, C and F). In the following MTT, Transwell migration, invasion, and adhesion experiment, it was found that si-Snail could significantly inhibit MCF-7/A cell invasion, migration and adhesion to HUVECs (Fig. 7D and E), while only slightly inhibited the survival of cells (Fig. 7A). Then we detected the protein levels of N-cadherin, CD44, and E-cadherin after Snail interference. We found that si-Snail could significantly down-regulate the protein level of N-cadherin and CD44, while up-regulate the level of E-cadherin (Fig. 7B). The above experiments indicated that suppression of Snail expression could inhibit the invasion, metastasis and adhesion of drug-resistant MCF-7/A cells.
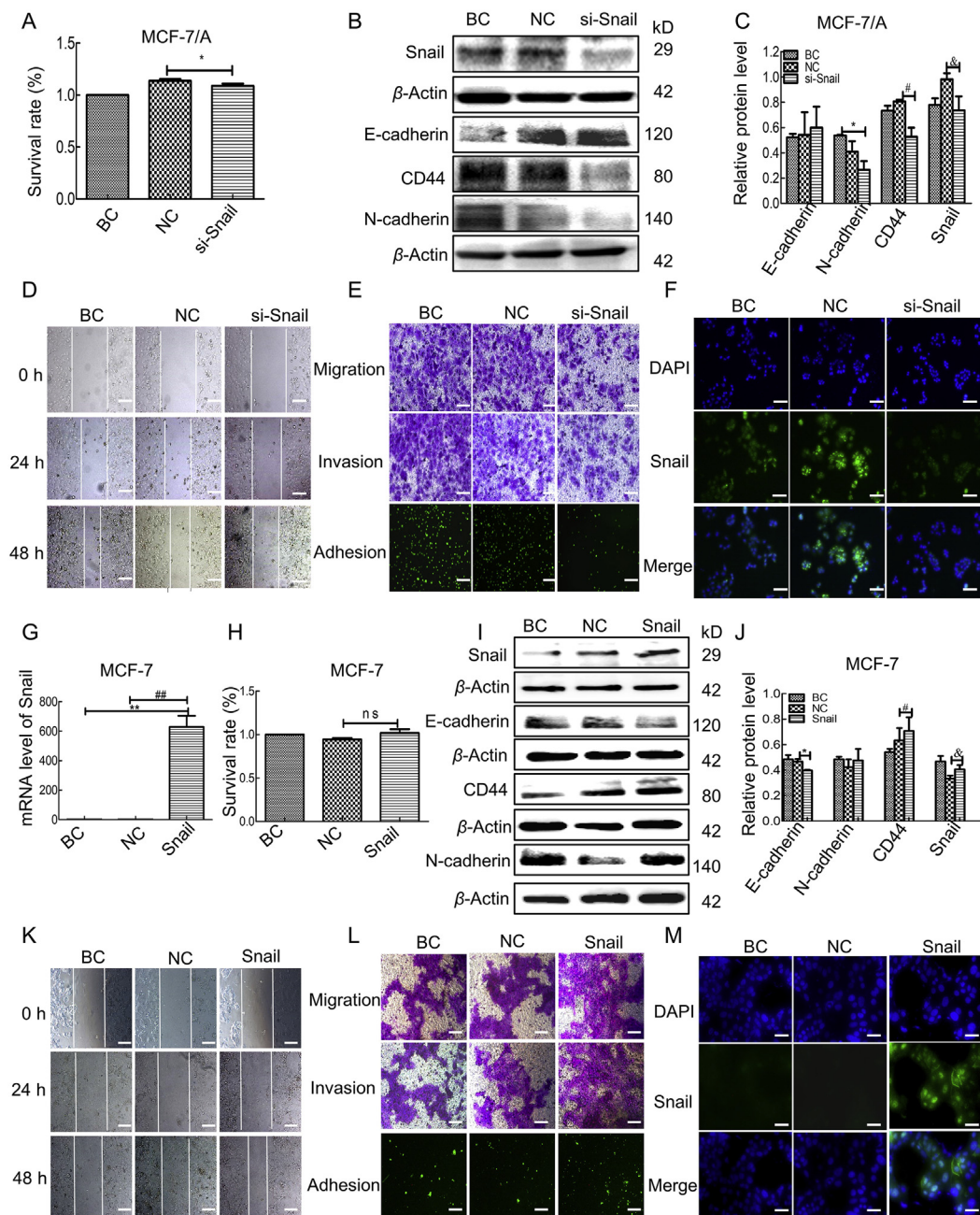
Figure 7 Knock down of Snail by siRNA inhibited the invasion, migration and adhesion to HUVECs of MCF-7/A cells while over-expression of Snail promoted the invasion, migration and adhesion of MCF-7 cells. BC: Blank control group, NC: Negative control group, si-Snail: Snail siRNA group, Snail: Snail over-expression group. (A) Cell viability of MCF-7/A cells cultured with si-Snail for 48 h was tested by MTT assay ($n = 3$). *$P < 0.05$ *vs.* NC. (B) The protein levels of N-cadherin, E-cadherin and Snail in MCF-7/A cells treated with si-Snail for 48 h were determined by Western blotting. (C) and (J) Statistical analysis of E-cadherin, N-cadherin, CD44 and Snail proteins was performed. *$P < 0.05$ *vs.* BC or NC, #$P < 0.05$, &$P < 0.05$ *vs.* NC. (D) The migration of MCF-7/A cells after incubation with si-Snail for 48 h was measured by wound scratch assay. (E) Transwell assay and cell adhesion assay were further employed to examine the migration, invasion and adhesion of MCF-7/A cells after incubation with Snail siRNA, respectively. (F) The protein level of Snail in MCF-7/A cells cultured with si-Snail for 48 h was observed by immunofluorescence assay. (G) The mRNA level of Snail in MCF-7 cells was determined by qRT-PCR. **$P < 0.01$ *vs.* BC, ##$P < 0.01$ *vs.* NC. (H) The cell survival rate after over-expression of Snail in MCF-7 cells was detected by MTT assay ($n = 3$). "ns" indicates no significance. (I) The expressions of Snail, N-cadherin and E-cadherin in MCF-7 cells were examined by Western blotting. (K) The migration of MCF-7 cells after over-expression of Snail was observed by scratch assay. (L) The invasion, migration and adhesion abilities of MCF-7 cells were detected by Transwell assay and adhesion assay. Bar = 20 μm. (M) Snail expression in MCF-7 cells was detected by immunofluorescence assay.

To further clarify the function of Snail in the migration, invasion in sensitive cancer cells, Snail was over-expressed by plasmid transfection in MCF-7 cells for 48 h. The successful high expression of Snail in sensitive MCF-7 cells was determined by qRT-PCR, immunofluorescence assay and Western blotting (Fig. 7G, I and M). Then the effects of over-expression of Snail on the growth, invasion, metastasis and adhesion of MCF-7 cells were observed. Results indicated that over-expression of Snail had no significant impact on the proliferation of MCF-7 cells (Fig. 7H); however, it could significantly promote their migration, invasion and adhesion with HUVECs (Fig. 7K and L). The promotion effect on the invasion and migration in MCF-7 cells after Snail over-expression might be related to the up-regulation of CD44, N-cadherin protein and down-regulation of E-cadherin protein (Fig. 7I).

3.8. Co-administration of miR34a and Dox down-regulated Notch/NF-κB and RAS/RAF/MEK/ERK pathway in MCF-7/A cells

Notch signaling pathway is known to be involved in the formation and progression of tumors through participating cell growth, apoptosis, invasion, adhesion and metastasis[13]. It has been reported that miR34a can directly target Notch to regulate the sensitivity of breast cancer cells to Dox[14]. At the same time, miR34a can also regulate the apoptosis and oxidative stress induced by visfatin through NF-κB pathway[15], indicating the correlation between miR34a and NF-κB. Therefore, we further examined the effects of miR34a and Dox combination on Notch/NF-κB signaling pathways. As shown in Fig. 8A, the expressions of Notch and Snail were abnormally activated in MCF-7/A cells. Both miR34a (100 nmol/L) and Dox (10 μmol/L) alone could reduce the protein level of Notch in MCF-7/A cells; moreover, a significant down-regulation of Notch was detected in the combination group. It was reported that Notch signaling pathway induced invasion and migration of MDA-MB-231 cells via up-regulating NF-κB transcriptional factor's activity[16]. Therefore, the effect of miR34a combination with Dox on NF-κB expression in MCF-7/A cells was examined. As displayed in Fig. 8A, either miR34a or Dox reduced the protein level of NF-κB in MCF-7/A cells and combination treatment of miR34a and Dox caused a stronger suppression effect than Dox alone. In order to further investigate whether Notch can regulate Snail expression via NF-κB, Notch inhibitor DAPT was introduced to detect the change of NF-κB and Snail expression. Results suggested that DAPT could down-regulate the protein expressions of Notch, NF-κB and Snail. In addition, for the combined miR34a and Dox group, DAPT could dose-dependently reduce the protein expressions of Notch, NF-κB and Snail. Furthermore, PDTC, an inhibitor of NF-κB, could also reduce the protein level of Snail in a dose-related pattern in MCF-7/A cells after co-administration with miR34a and Dox (Fig. 8D). These experiments suggested that Notch/NF-κB/Snail were regulated by miR34a and Dox in MCF-7/A cells.

RAS/RAF/MEK/ERK pathway also plays an indispensable role in regulating cell proliferation, differentiation, apoptosis, metastasis and metabolism[17]. It has been reported that miR34a not only regulates cell proliferation through PDGFR−β/RAS−MAPK signaling pathway in mesangial cells or by inhibiting MEK1 expression in K562 cells[18,19], but also regulates apoptosis of epithelial cells through RAS/RAF/MEK/ERK and PI3K/AKT/mTOR signaling pathways[20]. Therefore, we studied the effects of miR34a combined with Dox on RAS associated signaling pathways. Results suggested that administration of MCF-7/A cells

with Dox alone could significantly reduce the expression of p-ERK, pan-RAS and k-RAS, and treatment with miR34a alone could induce a significant decrease of pan-RAS and k-RAS. What's more, co-treatment of Dox and miR34a caused a synergistic down-regulation on the protein expressions of pan-RAS, RAF, k-RAS, p-ERK, p-MEK in MCF-7/A cells (Fig. 8B and C). To further verify whether RAS/RAF/MEK/ERK pathway could regulate the expression of Snail, RAS inhibitor salirasib and MEK inhibitor pimasertib was introduced to observe the changes of Snail expression. The results showed that for the combined group, pimasertib could reduce the level of MEK1/2, p-MEK1/2 and Snail in a dose-dependent pattern (Fig. 8D). Meanwhile, salirasib could decrease the expression of k-RAS and Snail in a dose-dependent pattern in the co-administration group. In all, the above data together indicated that co-administration of miR34 and Dox suppressed RAS/RAF/MEK/ERK signaling pathway in MCF-7/A cells.

3.9. Co-administration of miR34a and Dox suppressed tumor growth and metastasis in nude mice implanted with MCF-7/A cells by inhibiting Snail expression in vivo

The synergistic effect of miR34a and Dox on Dox-resistant breast cancer were evaluated by a mice xenograft model. The combination group significantly inhibited the MCF-7/A tumor growth in nude mice. Compared with the Control group, the co-administration group induced 55% tumor reduction, while Dox alone group resulted in 37.5% tumor reduction (Fig. 9A and D). The tumor suppression effect of the combination therapy was also verified by the slow increase in tumor volume (Fig. 9C). No remarkable changes of body weight or other responses in the mice were found between the combination group and Control group (Fig. 9B). Moreover, the expressions of Snail, BCL-2, BAX and cleaved PARP in tumor tissues were also detected. As displayed in Fig. 9E and F, co-administration of agomiR34a and Dox induced a distinct decrease of Snail and BCL-2/BAX and an increase of cleaved PARP in MCF-7/A xenografts compared with Dox group. What's more, the level of Snail in tumor xenografts was also further analyzed by immunofluorescence and immunohistochemical analysis (Fig. 9G and H), the results showed the protein level of Snail in combination group was clearly lower than that in Control group and Dox group, which was in accordance with the results of in vitro experiment. H&E staining was also employed to assess tumor growth, and it was found the pathological features of tumors for co-administration group were quite different from that of normal saline group. Apoptosis in different degree, a weakened nuclear staining and irregular shape were found in co-administration group (Fig. 9H). Taken together, these results indicate that up-regulation of miR34a combined with Dox significantly suppress the tumor growth which might be closely related to the down-regulation of Snail in MCF-7/A xenografts.

4. Discussion

Resistance towards chemotherapy has become a global challenge threatening human's health for patients with breast and other cancers. In particular, for BCa patients in the late stage due to single drug resistance, multi-drug resistance, distal metastasis and increased invasive ability are more easily to emerge[21]. Overcome drug resistance through inhibition metastasis related genes may provide an alternative strategy. Efforts have been
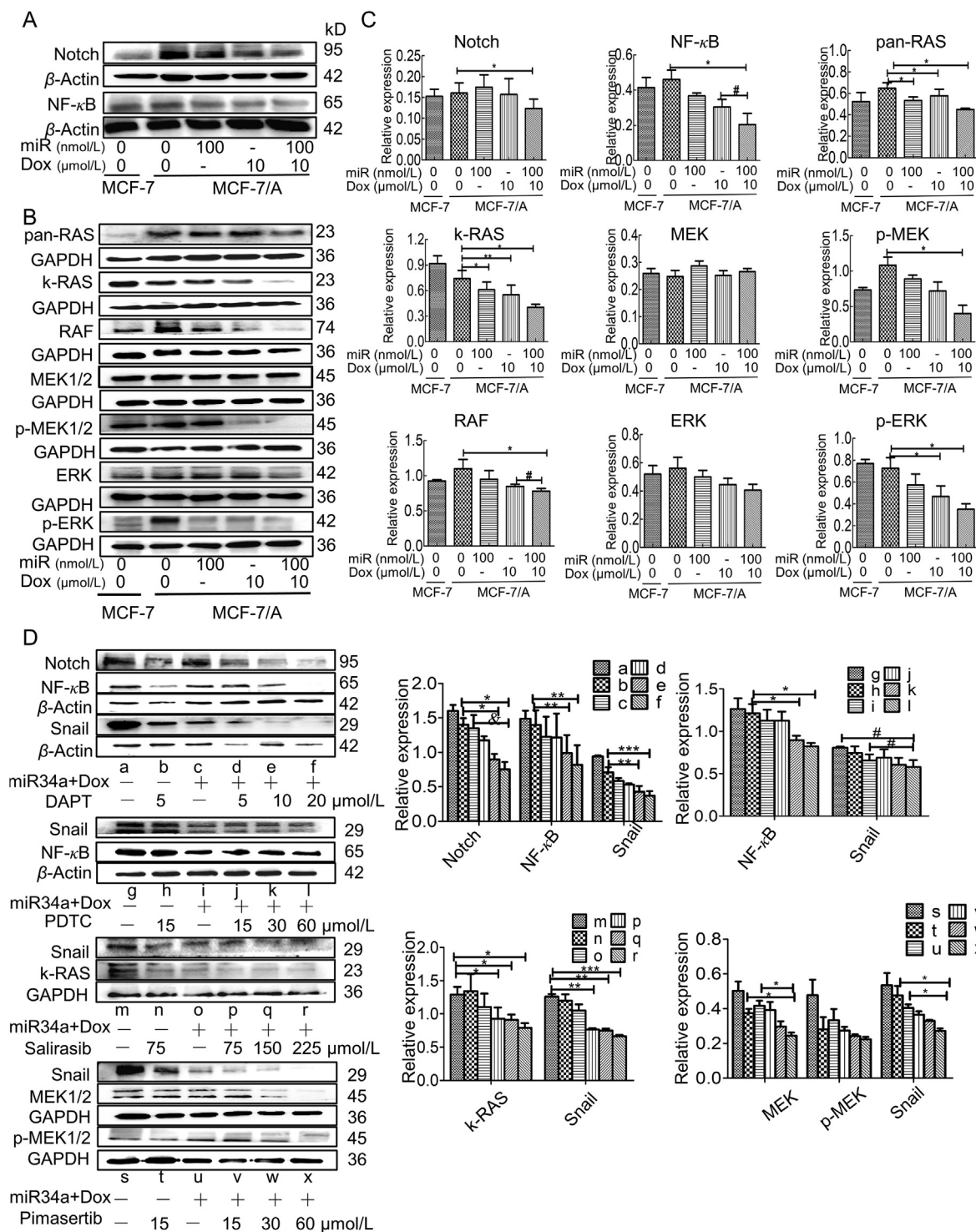
Figure 8 Co-administration of miR34a and Dox down-regulated Notch/NF-κB and RAS/RAF/MEK/ERK pathway in MCF-7/A cells. (A) The protein expressions of Notch and NF-κB were determined by Western blotting. (B) The levels of pan-RAS, k-RAS, RAF, MEK1/2, ERK, p-MEK1/2, p-ERK were determined by Western blotting assay. (C) Statistical analysis of protein expression of Notch, NF-κB, MEK1/2, p-MEK1/2, RAF, p-ERK, ERK, pan-RAS and k-RAS was performed ($n \geq 3$). *$P < 0.05$, **$P < 0.01$ vs. Untreated MCF-7/A control. [#]$P < 0.05$ vs. Dox alone. (D) Effects of Notch inhibitor DAPT, NF-κB inhibitor PDTC, k-RAS inhibitor salirasib and MEK inhibitor pimasertib at different concentrations on the pathway associated protein expression were determined by Western blotting assay ($n \geq 3$). *$P < 0.05$, **$P < 0.01$, ***$P < 0.001$; [#]$P < 0.05$; [&]$P < 0.05$. miR represents miR34a.
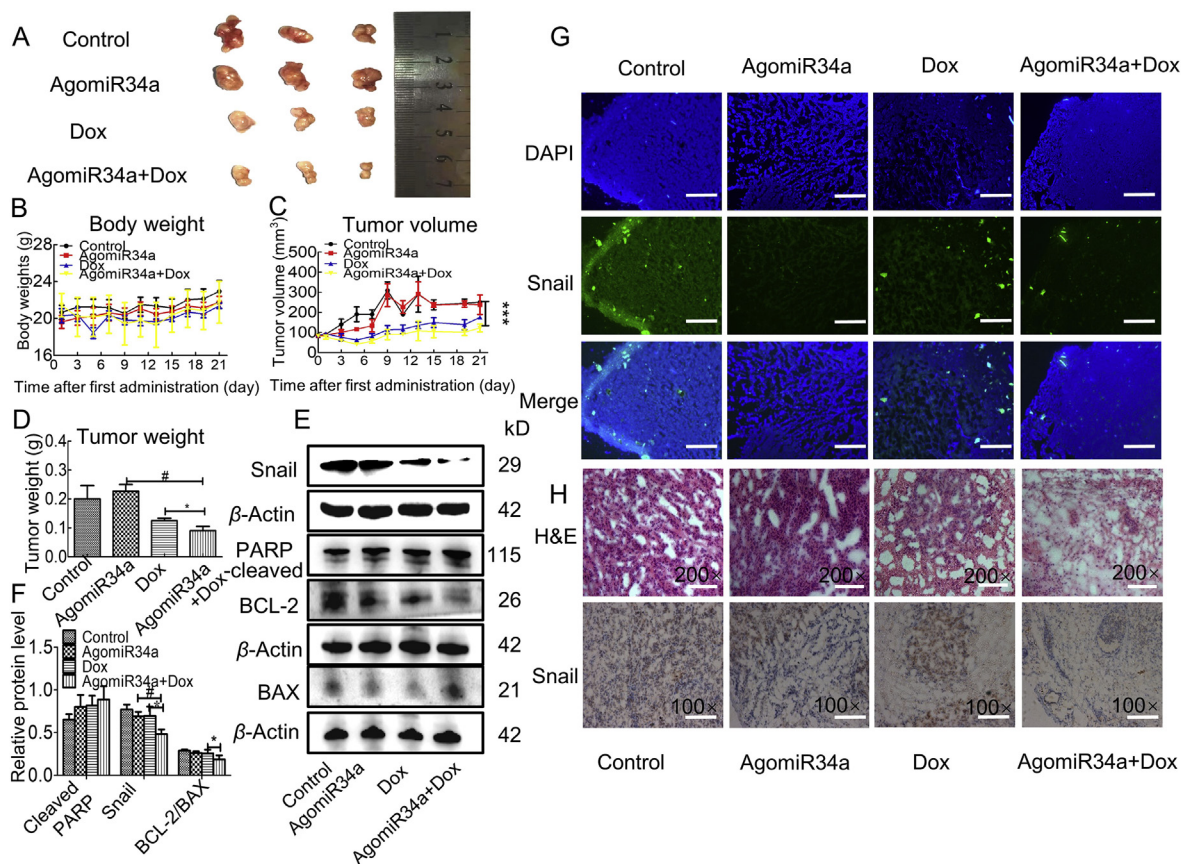
Figure 9 Combination of agomiR34a and Dox slowed down the xenograft growth of MCF-7/A cells *in vivo*. (A) Representative images of xenografts after administration of agomiR34a, Dox or agomiR34a combined with Dox for 21 days. (B) and (C) Body weight and tumor volume were determined every three days for 21 days ($n = 3$). ***$P < 0.001$ *vs.* Control. (D) After the experiment was over, nude mice were sacrificed and the tumor tissues were weighed. *$P < 0.05$ *vs.* Dox, #$P < 0.05$ *vs.* AgomiR34a. (E) The protein expressions of Snail, BCL-2, BAX and cleaved PARP in MCF-7/A tumor tissues were detected and analyzed using Western blotting ($n \geq 3$). (F) Statistical analysis of relative expression of cleaved PARP, Snail and the ratio of BCL-2/BAX was performed. *$P < 0.05$ *vs.* Dox, #$P < 0.05$ *vs.* AgomiR34a. (G) Expressions of Snail in tumor xenograft were analyzed by immunofluorescence assay. (H) H&E staining and immunohistochemical assay were performed for tumors in different groups. Scale bar = 20 μm.

devoted to find potential predictors and driver genes for improving therapeutic responses. miR34a is deemed to be a potent tumor-suppressor gene in different types of cancers[22–25], and exerts an important role among cell migration, invasion, proliferation, differentiation and immuno-regulation[26,27]. Recently, evidence suggested that miR34a is also correlated with drug resistance. However, the mechanism by which miR34a regulates Dox resistance and whether the combination of miR34a and chemotherapeutic drug could produce synergistic effects to inhibit tumor growth and metastasis still needs to be illustrated. In this study, we demonstrated that miR34a could directly target Snail to increase the sensitivity of Dox-resistant BCa cells (MCF-7/A) to Dox. miR34a combined with Dox down-regulated the expression of Snail through Notch/NF-κB and RAS/RAF/MEK/ERK pathway to produce a suppression on proliferation, migration, invasion, and apoptosis induction, thus reversing drug resistance of breast cancer MCF-7/A cells.

Firstly, combination use of miR34a and Dox could synergistically inhibit the growth of MCF-7/A cells with the highest reversal (7.54-

fold) induced by 100 nmol/L miR34a, so 100 nmol/L was chosen as the transfection concentration of miR34a in the combination treatment. At the same time, 10 μmol/L Dox for apoptosis assay, and 7 μmol/L Dox for invasion and migration assay were used in combination treatment to avoid the cytotoxic effect of Dox. We observed that combination of 100 nmol/L miR34a and 10 μmol/L Dox could clearly inhibit the survival and induce apoptosis of MCF-7/A cells by decreasing the ratio of BCL-2/BAX and increasing PARP expression which were related to the promotion of mitochondrial apoptosis pathway[28]. At the same time, interestingly, in comparison to parental sensitive MCF-7 cells, MCF-7/A cells showed an improved cell mobility, indicating drug resistant cells were more prone to migrate and invade due to an aggressive phenotype. Fortunately, the combination of miR34a and Dox could significantly ameliorate this trend, which may be associated with a decrease of N-cadherin and an increase of E-cadherin, thus indicating an inhibition toward EMT. Moreover, it's worth mentioning that this change was largely due to the introduction of miR34a.

EMT is a very complex stepwise pathological process that commonly existed in wound healing, embryonic development,
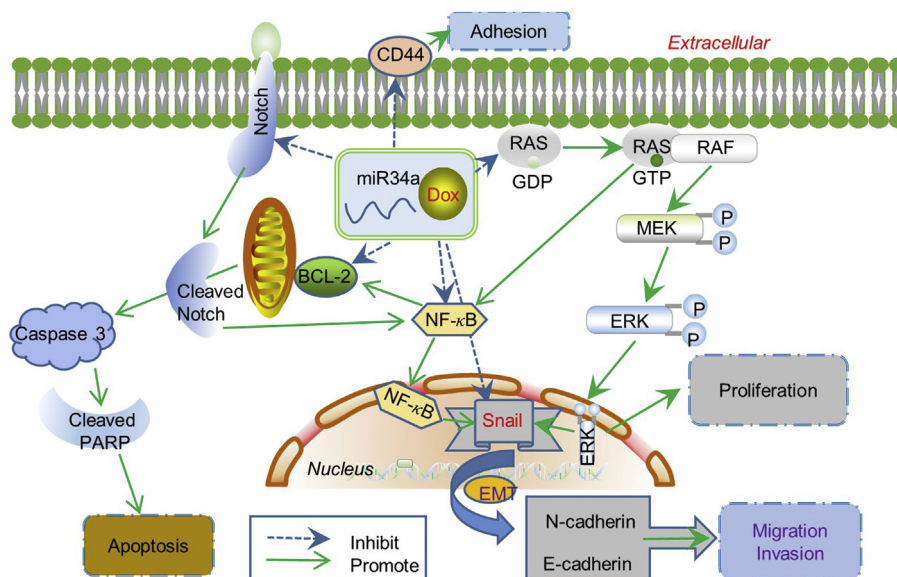
Figure 10   The proposed pathway of synergistic anti-tumor effects of miR34a and Dox in MCF-7/A cells.

organ fibrosis, and tumor metastasis[29−31]. It is reported that EMT can be modulated by stimulation of extracellular signals and activation of related transcription factors, such as TWIST1 (Twist-related protein 1), Snail, ZEB (zinc-finger E-box-binding), SLUG (zinc finger protein SNAI2), which are main moderators of the EMT program[32]. To further explore the molecular target of miR34a inhibiting EMT, target prediction using miRDB database and starbase software was performed. We found there existed a binding sequence between the 3′ UTR region of Snail and the seed region of miR34a (Fig. 6D), indicating Snail might be a direct target of miR34a. Then luciferase reporter gene detection system was further employed to verify the binding of miR34a with Snail. Moreover, we confirmed that miR34a could reduce Snail expression at protein and mRNA levels through binding with Snail at the 3′ UTR region directly.

Snail, the first discovered transcriptional regulator of E-cadherin, which plays a vital role in the process of EMT. It is reported that the expression of Snail in BCa is involved in tumor recurrence, metastasis and poor prognosis[33]. In the present study, we found that knock-down of Snail could suppress the invasion, migration of MCF-7/A cells and the adhesion to HUVECs, while over-expression of Snail could accelerate the invasion, migration and adhesion of MCF-7 cells, indicating that metastasis is more prone to happen in drug resistant cells. Furthermore, the combination of Dox and miR34a significantly reduced Snail expression in MCF-7/A cells *in vitro* and *in vivo*.

It has long been recognized that EMT related transcription factors (EMT-TFs) could facilitate the acquisition of resistance phenotypes[34]. And many ABC transporter genes have the promoter region that could bind with EMT-TFs; hence, the activation of EMT program could simultaneously increase drug resistance[35]. However, EMT-TFs can also induce drug resistance in other forms independent of ABC transporters, such as inducing apoptosis, cycle arrest or some other ways[36]. And Snail has also been reported to induce chemoresistance by increasing the expression of ABC binding members such as BCRP and P-GP or independently of ABC transporters[37]. In the present study, we demonstrated that the co-administration of miR34a and Dox could not distinctly reduce the expression of P-GP, MRP and GST-π. However, the

combination treatment could dramatically down-regulate the protein expressions of BCRP and TOP2A. BCRP is a specific ATP-binding cassette efflux transporter, whose high expression was related with multidrug resistance[38], and there is a high correlation between Snail and BCRP in breast cancer[39]. The down-regulation of BCRP induced by co-administration of Dox and miR34a might be caused by the introduction of miR34a, leading to a down-regulation of Snail[37]. TOP2A was a known target of Dox, which mediated the breaking and binding of DNA[40], and the level of miR34a was also correlated to TOP2A in BCa tissue samples[41]. Therefore, this makes sense why the decrease of TOP2A was more obvious in the combination group.

Notch related pathway is reported to be a highly conserved signaling pathway, whose imbalance is highly related to tumorigenesis, metabolism and cell differentiation. Recent studies showed that Notch related pathway might be participated in tumor drug resistance, through increasing the invasion and metastasis abilities of tumor cells[42]. In addition, evidence have shown that Notch signaling pathway also promote tumor progression through cross-talk with other carcinogenic pathways, such as mTOR, AKT, WNT, RAS, Androgen receptor and NF-κB[43]. It is reported that NF-κB could activate both mitochondrial (intrinsic) and death receptor (extrinsic) pathways to suppress cell apoptosis through up-regulating BCL-2 family[44]. Moreover, studies have shown that miR34a can target Notch to inhibit EMT progression[45]. In this study, we found that the protein level of Notch in MCF-7/A cells was distinctly increased and combination of miR34a and Dox significantly inhibited its expression. What's more, the protein level of NF-κB in the combination group was also significantly suppressed. Earlier reports showed Notch could regulate the expression of Snail through binding with Notch intracellular domain[46]. After Notch or NF-κB inhibitor (DAPT and PDTC) was introduced to inhibit the expression of Notch and NF-κB, Snail expression was significantly decreased, indicating that Notch/NF-κB signaling pathway could regulate Snail expression.

RAS/RAF/MEK/ERK pathway is a highly activated signaling pathway involved in regulating apoptosis, survival, metastasis and invasion[47]. It has been demonstrated that miR34a participated in the abnormal regulation of RAS/RAF/MEK/ERK pathway. For

example, miR34a suppressed RAS/RAF/MEK/ERK pathway through decreasing the expression of c-SRC in K-562 cells[48]. Furthermore, miR34a could inhibit cell survival through suppressing the RAS/RAF/MEK/ERK pathway in mesangial cells[18]. RAS, as a member of oncogene family, plays a key role in the control of cell growth and differentiation[49]. It mainly existed in three forms including n-RAS, h-RAS, and k-RAS (the most commonly activated member in cancer)[50]. In the present study, we found that pan-RAS is obviously activated in drug-resistant MCF-7/A cells. The co-administration of miR34a and Dox significantly reduced the protein level of k-RAS, pan-RAS, RAF, p-MEK, p-ERK and ERK. It is reported that Snail was a downstream effector of ERK pathway[51]. So RAS inhibitor (salirasib) and MEK inhibitor (pimasertib) were introduced to inhibit RAS/RAF/MEK/ERK pathway, then we observed that the relative expression of Snail was significantly reduced, indicating that RAS/RAF/MEK/ERK pathway involved in the drug resistance by up-regulating Snail expression. Therefore, we deduced that combination of miR34a and Dox inhibited Notch/NF-κB and RAS/RAF/MEK/ERK pathway, resulting in the down-regulation of Snail in MCF-7/A cells.

In addition, RAS-dependent signaling pathways can regulate gene expression through activation of transcription factors, such as activation of NF-κB[52]. Previous studies have reported that RAS oncoprotein could target trans-activation region in the P65 subunit of NF-κB to regulate the transcriptional activity of NF-κB, thereby regulating cell apoptosis[53]. RAS could also activate NF-κB through PI3K-AKT-dependent pathway to mediate cell survival[54], resulting in up-regulating genes involved in apoptosis and proliferation. It is reported that the aberrant activation of Notch pathway is a common early event in breast cancer[55]. However, interactions between the Notch and RAS signaling pathways have always remain controversial for many years, which are reported to produce cooperative or antagonistic effects depending on specific contexts[56]. In the present study, we found both RAS and Notch related proteins were abnormally activated in Dox resistant MCF-7/A cells, nevertheless they were significantly suppressed after treatment of miR34a and Dox, which indicated similar effects existed between Notch and RAS pathway in Dox resistant breast cancer cells. The proposed synergistic anti-tumor mechanism of Dox and miR34a was summarized in Fig. 10.

In conclusion, miR34a combined with Dox synergistically inhibited the survival, invasion and metastasis, and promoted apoptosis of Dox-resistant breast cancer MCF-7/A cells *in vitro* and *in vivo*. The underlying mechanism was related to the down-regulation of Snail directly and through Notch/NF-κB and RAS/RAF/MEK/ERK pathways. The research provides an experimental basis for miR as an adjuvant agent to enhance the sensitivity of chemotherapeutic drugs clinically. The combined use of miR34a and Dox has a desirable potential for treatment on Dox-resistant breast cancer, especially for patients with advanced metastasis.

Acknowledgments

Author contributions

Xiaoxia Yang and Xiuli Guo designed the research, wrote and revised the manuscript. Xiaoxia Yang, Pengfei Shang, Bingfang Yu performed most of the experiment. Qiuyang Jin, Jing Liao, Lei Wang, Jianbo Ji participated the animal experiments. All authors have read and approved the final manuscript.

Conflicts of interest

The authors claim that the researchers in this study have no conflict of interest.

Appendix A. Supporting information

Supporting data to this article can be found online at https://doi.org/10.1016/j.apsb.2021.06.003.

References

1. Coley HM. Mechanisms and strategies to overcome chemotherapy resistance in metastatic breast cancer. *Cancer Treat Rev* 2008;**34**:378−90.
2. Chang L, Hu Y, Fu Y, Zhou T, You J, Du J, et al. Targeting slug-mediated non-canonical activation of c-Met to overcome chemoresistance in metastatic ovarian cancer cells. *Acta Pharm Sin B* 2019;**9**:484−95.
3. Zheng WP, Li MH, Lin YX, Zhan X. Encapsulation of verapamil and doxorubicin by MPEG-PLA to reverse drug resistance in ovarian cancer. *Biomed Pharmacother* 2018;**108**:565−73.
4. Kumar A, Jaitak V. Natural products as multidrug resistance modulators in cancer. *Eur J Med Chem* 2019;**176**:268−91.
5. Liang GF, Zhu YL, Ali DJ, Tian T, Xu HT, Si K, et al. Engineered exosomes for targeted co-delivery of miR-21 inhibitor and chemotherapeutics to reverse drug resistance in colon cancer. *J Nanobiotechnol* 2020;**18**:10.
6. Liang L, Fu J, Wang S, Cen H, Zhang L, Mandukhail SR, et al. MiR-142-3p enhances chemosensitivity of breast cancer cells and inhibits autophagy by targeting HMGB1. *Acta Pharm Sin B* 2020;**10**:1036−46.
7. Gabriella M, Maria Teresa DM, Giuseppe DR, Ahmad FA, Angela L, Virginia C, et al. MiR-34: a new weapon against cancer?. *Mol Ther Nucleic Acids* 2014;**3**:195.
8. Zhang Q, Zhuang JL, Deng YM, Yang L, Cao WM, Chen W, et al. MiR34a/GOLPH3 axis abrogates urothelial bladder cancer chemoresistance *via* reduced cancer stemness. *Theranostics* 2017;**19**:4777−90.
9. Chalanqui MJ, O'Doherty M, Dunne NJ, McCarthy HO. MiRNA 34a: a therapeutic target for castration-resistant prostate cancer. *Expert Opin Ther Targets* 2016;**20**:1075−85.
10. Wang L, Li YS, Yu LG, Zhang XK, Zhao L, Gong FL, et al. Galectin-3 expression and secretion by tumor-associated macrophages in hypoxia promotes breast cancer progression. *Biochem Pharmacol* 2020;**178**:114113.
11. Yu LG, Andrews N, Zhao QC, McKean D, Williams JF, Connor LJ, et al. Galectin-3 interaction with Thomsen-Friedenreich disaccharide on cancer associated MUC1 causes increased cancer cell endothelial adhesion. *J Biol Chem* 2007;**282**:773−81.
12. Li T, Wang SL, Hao JB, Zhang Y, Hu R, Liu XQ, et al. MiR-451a attenuates doxorubicin resistance in lung cancer *via* suppressing epithelial−mesenchymal transition (EMT) through targeting c-Myc. *Biomed Pharmacother* 2020;**125**:109962.
13. Lobry C, Oh P, Mansour MR, Look AT, Aifantis I. Notch signaling: switching an oncogene to a tumor suppressor. *Blood* 2014;**123**:2451−9.

14. Li XJ, Ji MH, Zhong SL, Zha QB, Xu JJ, Zhao JH, et al. MicroRNA-34a modulates chemosensitivity of breast cancer cells to adriamycin by targeting notch1. *Arch Med Res* 2012;**43**:514−21.

15. Cheleschi S, Tenti S, Mondanelli N, Corallo C, Barbarino M, Giannotti S, et al. MicroRNA-34a and microRNA-181a mediate visfatin-induced apoptosis and oxidative stress *via* NF-κB pathway in human osteoarthritic chondrocytes. *Cells* 2019;**8**:874.

16. Li L, Zhang J, Xiong NY, Li S, Chen Y, Yang H, et al. Notch-1 signaling activates NF-kappa B in human breast carcinoma MDA-MB-231 cells *via* PP2A-dependent AKT pathway. *Med Oncol* 2016;**33**:33.

17. Freeman AK, Morrison DK. Mechanisms and potential therapies for acquired resistance to inhibitors targeting the Raf or MEK kinases in cancer. In: *Molecular mechanisms of tumor cell resistance to chemotherapy.* New York: Springer; 2013. p. 47−67.

18. Chen DP, Li Y, Mei Y, Geng WJ, Yang JR, Hong Q, et al. miR-34a regulates mesangial cell proliferation *via* the PDGFR-β/Ras-MAPK signaling pathway. *Cell Mol Life Sci* 2014;**71**:4027−42.

19. Liu XR, Zhang L, Yang LC, Cui JZ, Che SC, Liu YX, et al. miR-34a/c induce caprine endometrial epithelial cell apoptosis by regulating circ-8073/CEP55 *via* the RAS/RAF/MEK/ERK and PI3K/AKT/mTOR pathways. *J Cell Physiol* 2020;**235**:10051−67.

20. Ichimura A, Ruike Y, Terasawa K, Shimizu K, Tsujimoto G. Micro-RNA-34a inhibits cell proliferation by repressing mitogen-activated protein kinase kinase 1 during megakaryocytic differentiation of K562 cells. *Mol Pharmacol* 2010;**77**:1016−24.

21. Mohajeri M, Sahebkar A. Protective effects of curcumin against doxorubicin-induced toxicity and resistance: a review. *Crit Rev Oncol Hematol* 2018;**122**:30−51.

22. Li YQ, Guessous F, Zhang Y, Dipierro C, Kefas B, Johnson E, et al. MicroRNA-34a inhibits glioblastoma growth by targeting multiple oncogenes. *Cancer Res* 2009;**69**:7569−76.

23. Park EY, Chang ES, Lee EJ, Lee HW, Kang HG, Chun KH, et al. Targeting of miR34a−Notch1 axis reduced breast cancer stemness and chemoresistance. *Cancer Res* 2014;**74**:7573−82.

24. Liu C, Kelnar K, Liu BG, Chen X, Calhoun-Davis T, Li HW, et al. The microRNA miR-34a inhibits prostate cancer stem cells and metastasis by directly repressing CD44. *Nat Med* 2011;**17**:211−5.

25. Gallardo E, Navarro A, Viñolas N, Marrades RM, Diaz T, Gel B, et al. miR-34a as a prognostic marker of relapse in surgically resected non-small-cell lung cancer. *Carcinogenesis* 2009;**30**:1903−9.

26. Yan K, Gao J, Yang TT, Ma Q, Qiu XC, Fan QY, et al. MicroRNA-34a inhibits the proliferation and metastasis of osteosarcoma cells both *in vitro* and *in vivo*. *PLoS One* 2012;**7**:e33778.

27. Kurowska-Stolarska M, Alivernini S, Melchor EG, Elmesmari A, Tolusso B, Tange C, et al. MicroRNA-34a dependent regulation of AXL controls the activation of dendritic cells in inflammatory arthritis. *Nat Commun* 2017;**8**:15877−91.

28. Kehr S, Haydn T, Bierbrauer A, Irmer B, Vogler M, Fulda S. Targeting BCL-2 proteins in pediatric cancer: dual inhibition of BCL-XL and MCL-1 leads to rapid induction of intrinsic apoptosis. *Cancer Lett* 2020;**482**:19−32.

29. Pastushenko I, Blanpain C. EMT transition states during tumor progression and metastasis. *Trends Cell Biol* 2019;**29**:212−26.

30. Nordin A, Sainik NQAV, Zulfarina MS, Naina-Mohamed I, Saim A, Idrus RBH, et al. Honey and epithelial to mesenchymal transition in wound healing: an evidence-based review. *Wound Med* 2017;**18**:8−20.

31. Bakir B, Chiarella AM, Pitarresi JR, Rustgi AK. EMT, MET, Plasticity, and tumor metastasis. *Trends Cell Biol* 2020;**30**:764−76.

32. Lamouille S, Xu J, Derynck R. Molecular mechanisms of epithelial-mesenchymal transition. *Nat Rev Mol Cell Biol* 2014;**15**:178−96.

33. Peinado H, Olmeda D, Cano A. SNAIL, Zeb and bHLH factors in tumour progression: an alliance against the epithelial phenotype?. *Nat Rev Cancer* 2007;**7**:415−28.

34. Goossens S, Vandamme N, Vlierberghe PV, Berx G. EMT transcription factors in cancer development re-evaluated: beyond EMT and MET. *Biochim Biophys Acta Rev Cancer* 2017;**1868**:584−91.

35. Xin H, Kong Y, Jiang XX, Wang K, Qin XR, Miao ZH, et al. Multi-drug-resistant cells enriched from chronic myeloid leukemia cells by

36. Doxorubicin possess tumor-initiating-cell properties. *J Pharmacol Sci* 2013;**122**:299−304.

36. Li R, Wu CL, Liang HY, Zhao YH, Lin CY, Zhang XJ, et al. Knockdown of TWIST enhances the cytotoxicity of chemotherapeutic drugs in doxorubicin-resistant HepG2 cells by suppressing MDR1 and EMT. *Int J Oncol* 2018;**53**:1763−73.

37. Erin N, Grahovac J, Brozovic A, Efferth T. Tumor microenvironment and epithelial mesenchymal transition as targets to overcome tumor multidrug resistance. *Drug Resist Updat* 2020;**53**:100715.

38. Jia H, Yang Q, Wang T, Cao Y, Jiang QY, Ma HD, et al. Rhamnetin induces sensitization of hepatocellular carcinoma cells to a small molecular kinase inhibitor or chemotherapeutic agents. *Biochim Biophys Acta* 2016;**1860**:1417−30.

39. Chen WJ, Wang H, Tang Y, Liu CL, Li HL, Li WT. Multidrug resistance in breast cancer cells during epithelial−mesenchymal transition is modulated by breast cancer resistant protein. *Chin J Cancer* 2010;**29**:151−7.

40. Lyu YL, Kerrigan JE, Lin CP, Azarova AM, Tsai YC, Ban Y, et al. Topoisomerase IIbeta mediated DNA double-strand breaks: implications in doxorubicin cardiotoxicity and prevention by dexrazoxane. *Cancer Res* 2007;**67**:8839−46.

41. Li ZH, Weng X, Xiong QY, Tu JH, Xiao A, Qiu W, et al. miR-34a expression in human breast cancer is associated with drug resistance. *Oncotarget* 2017;**63**:106270−82.

42. Zhou W, Wang G, Guo S. Regulation of angiogenesis *via* Notch signaling in breast cancer and cancer stem cells. *Biochim Biophys Acta* 2013;**1836**:304−20.

43. Wang ZW, Li YW, Ahmad A, Azmi AS, Banerjee S, Kong D, et al. Targeting Notch signaling pathway to overcome drug resistance for cancer therapy. *Biochim Biophys Acta* 2010;**1806**:258−67.

44. Zinatizadeh MR, Schock B, Chalbatani GM, Zarandi PK, Jalali SA, Miri SR, et al. The nuclear factor kappa B (NF-κB) signaling in cancer development and immune diseases. *Genes Dis* 2020;**8**:287−97.

45. Han RF, Hao P, Wang LM, Li J, Shui SS, Wang YC, et al. MicroRNA-34a inhibits epithelial−mesenchymal transition of lens epithelial cells by targeting Notch1. *Exp Eye Res* 2019;**185**:107684.

46. Sahlgren C, Gustafsson MV, Jin SB, Poellinger L, Lendahl U. Notch signaling mediates hypoxia-induced tumor cell migration and invasion. *Proc Natl Acad Sci U S A* 2008;**105**:6392−7.

47. Mccubrey JA, Steelman LS, Chappell WH, Wong EWT, Chang FM, et al. Roles of the Raf/MEK/ERK pathway in cell growth, malignant transformation and drug resistance. *Biochim Biophys Acta* 2007;**177**:1263−84.

48. Yang Y, Ding L, Guo ZK, Zheng XL, Wang LS, Sun HY, et al. The epigenetically-regulated miR-34a targeting c-SRC suppresses RAF/MEK/ERK signaling pathway in K-562 cells. *Leuk Res* 2017;**55**:91−6.

49. Murugan AK, Grieco M, Tsuchida N. RAS mutations in human cancers: roles in precision medicine. *Semin Cancer Biol* 2019;**59**:23−35.

50. Khan I, Rhett JM, O'Bryan JP. Therapeutic targeting of RAS: new hope for drugging the "undruggable". *Biochim Biophys Acta Mol Cell Res* 2020;**1867**:118570.

51. Pradhan N, Parbin S, Kar S, Das L, Kirtana R, Seshadri S, et al. Epigenetic silencing of genes enhanced by collective role of reactive oxygen species and MAPK signaling downstream ERK/SNAIL axis: ectopic application of hydrogen peroxide repress *CDH1* gene by enhanced DNA methyltransferase activity in human breast cancer. *Biochim Biophys Acta Mol Basis Dis* 2019;**1865**:1651−65.

52. Mayo MW, Norris JL, Baldwin AS. Ras regulation of NF-kappa B and apoptosis. *Methods Enzymol* 2001;**333**:73−87.

53. Mayo MW, Wang CY, Cogswell PC, Rogers-Graham KS, Lowe SW, Der CJ, et al. Requirement of NF-κB activation to suppress P53-independent apoptosis induced by oncogenic Ras. *Science* 1997;**278**:1812−5.

54. Madrid LV, Wang CY, Guttridge DC, Schottelius AJ, Baldwin AS. Akt suppresses apoptosis by stimulating the transactivation potential of the RelA/p65 subunit of NF-κB. *Mol Cell Biol* 2000;**20**:1626−38.

55. Mittal S, Subramanyam D, Dey D, Kumar RV, Rangarajan A. Cooperation of Notch and Ras/MAPK signaling pathways in human breast carcinogenesis. *Mol Cancer* 2009;**23**:128.

56. Sundaram MV. The love-hate relationship between Ras and Notch. *Genes Dev* 2005;**19**:1825−39.